Optical Properties of Polystyrene and Polyarylate Block Copolymer and Their Control by Morphology Generation

HIROSHI OHISHI,[1] SOUICHIRO KISHIMOTO,[2] TOSHIO NISHI[3]

[1] Advanced Technology Research Laboratories, Nippon Steel Corporation, 3-35-1 Ida Nakahara-ku, Kawasaki 211, Japan

[2] Research & Development Center, Plastics Department, Unitika Corporation, Uji, Kozakura, Kyoto 611, Japan

[3] Department of Applied Physics, School of Engineering, The University of Tokyo, 7-3-1 Hongo, Bunkyo-ku, Tokyo 113, Japan

ABSTRACT: Relationship between phase morphology and optical properties of polystyrene and polyarylate (PS-PAr) block copolymers synthesized from telechelic polystyrene has been investigated. In the PS-PAr block copolymers, the PAr domains with higher melt viscosity were dispersed in the PS phase matrix with lower melt viscosity over the wide range of their composition from PS/PAr = 25/75 to 75/25 (wt ratio). The PAr domain size was dependent on the reactive ratio of PAr determined analogously by the mole fraction of the fed telechelic polystyrene. By controlling the mole fraction of the telechelic polystyrene more than 0.016 in synthesizing the PS-PAr block copolymer, the size of PAr domains could be reduced to the microscopic scale (smaller than 100 nm). Then, the PS-PAr block copolymers exhibited almost the same transparency as PAr in spite of the large difference in the refractive index between the PS and the PAr phase. Birefringence free condition for the PS-PAr block copolymers was determined by not only the PS/PAr composition but also the balance in the degree of molecular orientation of these chains. The latter factor suggests that PS and PAr chains undergo inhomogeneous stress and relaxation history during the injection process. By controlling Mn (number average molecular weight) and weight fraction of the fed OH-PS-OH around 20 000 and 55 wt %, respectively, in the synthesis of the PS-PAr block copolymer, the PS-PAr block copolymer exhibited almost zero birefringence without any sacrifice of transparency. Because in the PS-PAr block copolymer low birefringence and high transparency can coexist by controlling the adequate feeding condition in the synthesis process, the PS-PAr block copolymer would be a promising material for optical applications, such as a substrate of optical disks or optical lenses. © 2000 John Wiley & Sons, Inc. J Appl Polym Sci 78: 953–961, 2000

Key words: polystyrene; polyarylate; block copolymer; phase morphology; birefringence; transparency

INTRODUCTION

In recent years, use of amorphous polymers for optical applications has been increasing compared with inorganic glasses. Polymeric materials, however, usually exhibit a specific residual birefringence due to anisotropy in molecular segments.[1] The birefringence of polymeric materials is amplified during their processing, such as injection molding or extrusion, because in these processing molecular chains are oriented by flow and are not fully relaxed in the cooling stage. This

---

birefringence, which is named "molecular orientation birefringence," often leads to a fatal defect when applying polymeric materials to optical applications.[2] For example, in an application to magnetic optical disk, the residual birefringence of the substrate induces the noise in reading the recorded memories.[2–8] Further, in an application to optical lenses, the residual birefringence causes the focus aberrations. Thus, reducing the residual birefringence is one of the key factors in developing a new polymer for optical applications.

We have carried out research and development on polystyrene and polyarylate (PS-PAr) block copolymers aiming at optical application.

Polyarylate (PAr) is a polyester of bisphenol A and mixture of terephthalic acid/isophthalic acid (1 : 1 mole ratio). PAr is known as a high-performance polymer with excellent transparency, thermal stability, mechanical properties, and UV light stability.[9] However, PAr is poor in moldability mainly due to its high melt viscosity. Furthermore, because PAr has phenyl groups with high polarizability in its backbone, PAr shows positive birefringence due to residual molecular orientation after injection molding.[10]

Polystyrene (PS) is a transparent polymer with excellent moldability and has phenyl groups in the side chain, which generate negative stress-induced birefringence.

The focus of our research is to compensate their different birefringence without sacrificing transparency and produce a transparent polymer with good moldability and low birefringence. However, PAr and PS are immiscible,[11] so the simple mechanical blending of these polymers makes it difficult to control domain structure on a microscopic level. Microscopic control of domain size and distribution is necessary. To obtain a transparent resin, the domain should be reduced to much smaller size than the wavelength of visible light. In this sense, incorporation of chemical bonds between PAr and PS molecules is a good candidate.[12] In our earlier publications, we have reported a novel synthetic route of the PS and PAr block copolymer utilizing telechelic carboxyl terminated polystyrene,[13,14] and also revealed the relationship between the polymerization kinetics and the chain consequence of the PS and PAr block copolymers.[15] However, the relationship between the phase morphology and the optical properties of the PS-PAr block copolymers has not been fully investigated.

The purpose of this article is to make clear the relationship between the phase morphology and

(Step 1) Preparation of COOH-PS-COOH
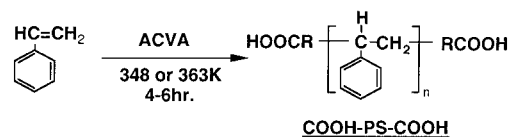
(Step 2) Conversion of carboxyl groups of COOH-PS-COOH into phenol groups
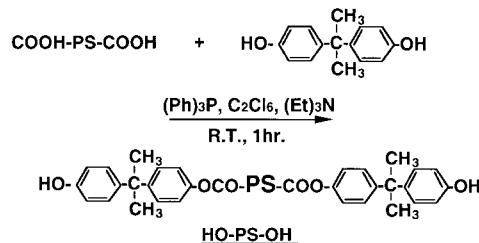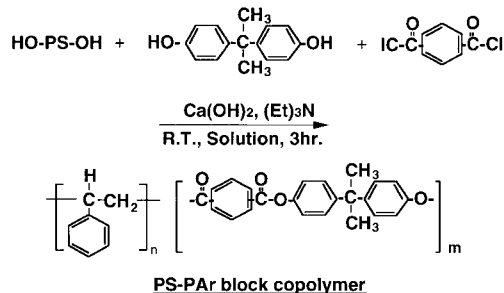
(Step 3) Synthesis of PS-PAr block copolymer

Figure 1   Reaction scheme.

the optical properties of PS-PAr block copolymer and to discuss how to synthesize a new birefringence-free PS-PAr block copolymer without sacrificing transparency.

EXPERIMENTS

PS-PAr block copolymers were synthesized (Fig. 1), and characterized in Table I according to the procedure described previously.[13,14] The PS-PAr block copolymers were injection molded at 553K by Mini-Max Injection Molder (Model CS-183, Custom Science Instruments, Inc., USA). Plates, 10 W × 30 L × 1.2 H mm, were prepared for the test specimens to analyze the phase morphology, transparency, and birefringence. The phase morphologies of the plate specimens were observed by transmission electron microscope (TEM) with the ruthenium tetraoxide staining technique. Ultrathin sections of about 35 nm were cut normal to

Table I The Block Copolymerization Conditions and the Results

| | Experimental Conditions of the Step 3 | | | The Block Copolymerization Results | | | | | | | | | | |
| | Feed | | Mol Fraction of OH-PS-OH to BPA | Pure PS-PAr Blockcopolymer | | | Homo-PAr | | | Unreacted OH-PS-OH | | | Block Copolymerization Rat | |
Sample Run No.	Mn of OH-PS-OH	Weight Composition (PS/PAr)		Mn	Mw	wt %	Mn	Mw	wt %	Mn	Mw	wt %	OH-PS-OH (%)	PAr (%)
950	9000	50/50	0.0398	—	—	—	—	—	—	8000	14 000	4.0	92	—
				(40 000)	(71 000)	(85)	(11 000)	(21 000)	(10.5)	(—)	(—)	(4.5)	(91)	(79)
960	9000	60/40	0.0597	—	—	—	—	—	—	9000	16 000	11.3	82	84
970	9000	70/30	0.0928	—	—	—	8000	11 000	4.8	—	—	—	—	
				(45 000)	(75 000)	(87)	(6700)	(10 000)	(2.6)	(—)	(—)	(10.5)		(96)
2140	21 000	40/60	0.0119	35 000	71 000	68	13 000	25 000	22	28 000	62 000	10	83	63
				(49 000)	(89 000)	(65)	(16 500)	(39 000)	(30)	(—)	(—)	(5)	(92)	(50)
2145	21 000	45/55	0.0146	40 000	75 000	60	10 000	22 000	32	27 000	63 000	6	87	42
2150	21 000	50/50	0.0179	35 000	80 000	69	10 000	20 000	27	31 000	74 000	4	92	47
				(55 000)	(87 000)	(72)	(14 000)	(24 000)	(22)	(—)	(—)	(6.6)	(87)	(56)
2155	21 000	55/45	0.0219	38 000	78 000	72	10 000	22 000	18	27 000	63 000	10	82	60
2160	21 000	60/40	0.0269	44 000	83 000	74	14 000	24 000	13	26 000	60 000	13	78	67
				(58 000)	(86 000)	(75)	(11 000)	(18 000)	(14)	(—)	(—)	(10)	(83)	(67)
5025	50 000	25/75	0.0024	—	—	—	—	—	—	53 000	140 000	2.6	90	—
				(—)	(—)	(39)	(23 000)	(42 000)	(58)	(—)	(—)	(2.7)	(89)	(22)
5050	50 000	50/50	0.0072	62 000	142 000	45.8	12 000	20 000	40.1	76 000	189 000	14.1	71	19.8
5060	50 000	60/40	0.0107	80 000	150 000	62.1	12 000	23 000	23.9	76 000	189 000	14	77	22.5
5075	50 000	75/25	0.0215	—	—	—	6700	8500	15.6	—	—	—	—	37.6
				(—)	(—)	(64.3)	(7900)	(13 000)	(11.3)	(—)	(—)	(24.4)	(67)	(55)

The first two digits of each sample corresponds to Mn of the fed OH-PS-OH used in step 3, and the last two digits correspond to weight fraction of the fed OH-PS-OH. The simulation results are shown in the parentheses. The data impossible to obtain experimentally owing to the limitation of the purification method are shown by the blank.

the longitudinal direction of the plate specimens by an ultra microtome (LKB Instruments Inc., Bromma, Sweden). The dark portions in the micrographs define the polystyrene phase, which is selectively stained by ruthenium tetraoxide. The TEM micrographs were analyzed by the digital image analysis (DIA). The transparency of the plate specimens was measured spectroscopically by using the light source with 800 nm wavelength, which was the same as the laser beam wavelength used in the optical memory storage systems. The birefringence was measured with polarized microscope equipped with a Senalmon type compensator.

To analyze the properties for practical use, the PS-PAr block copolymers were injection molded without any purification pretreatment such as cyclohexane or 1,1,1,3,3,3-hexafluoro-2-propanol extraction.[13,14]

RESULTS AND DISCUSSION

Polymerization

The experimental polymerization and the kinetic simulation model[14] results are shown in Table I. In spite of relatively high block copolymerization ratio of the fed HO-PS-OH (more than 70%), each sample contains unreacted homo-PS and homo-PAr as the byproducts of step 3 in Figure 1.

Phase Morphologies of the PS-PAr Block Copolymers

From the results of Table I, the PS-PAr block copolymers, synthesized by the scheme shown in Figure 1, are ternary polymer blends: pure PS-PAr block copolymer, homo-PS, and homo-PAr. These PS-PAr block copolymers undergo phase separation in microscopic, macroscopic, or both scale corresponding to chemical conditions of blending such as the molecular weight or the weight fraction of each component.[16] To analyze the effect of the molecular weight of the fed OH-PS-OH, run 0950, 2150, and 5050 are investigated. To analyze the effect of the fed composition of step 3, run 5025, 5050, and 5075 are investigated. In the following analysis, the size of PAr domains are estimated by the major axis of the equivalent ellipsoid.
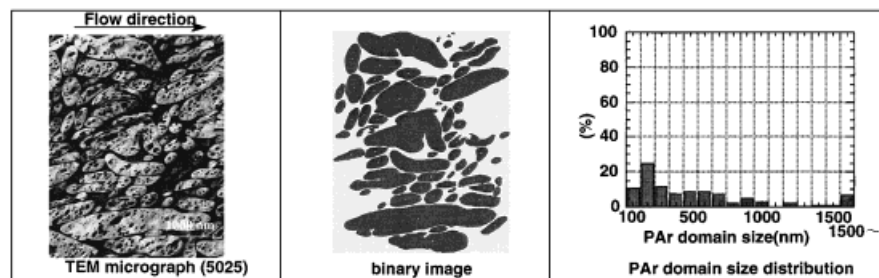
Figure 2 shows the TEM micrographs, binary images, and the PAr domain size distribution for run 0950 and 2150. Figure 3 gives those of run 5075, 5050, and 5025. In each sample, the PAr domains with higher melt viscosity are dispersed in the PS matrix with lower melt viscosity. The morphologies of run 0950 and 2150 look the same, and show phase separation in microscopic scale. Domain sizes are smaller than 100 nm and no macroscopic (larger than 100 nm) PAr domains are observed. There is a subtle size difference between run 0950 and 2150. The size distribution of the PAr domains of run 2150 is broader and shifted towards larger side. On the other hand, the morphologies of run 5075, 5050, and 5025 are quite different from those of run 0950 and 2150. They undergo phase separation in both microscopic and macroscopic scale. In the large PAr domains, the PS domains are dispersed in microscopic scale. These domains are formed by the PS segments of pure PS-PAr block copolymer dissolved in the homo-PAr phases. The ratio of larger size PAr domains increases in the order of run 5075, 5050, and 5025. For run 5025, more than 90% of PAr domains are dispersed in macroscopic scale.

This difference of the PAr domain size in large scale is due to the difference of the weight fraction of the constituents in the PS-PAr block copolymers as shown in Figure 4. In Figure 4, the constituent weight fraction of run 0950, 5075, and 5025 were estimated by the kinetic simulation results,[15] because they are impossible to be analyzed experimentally owing to the limitation of the purification method.[13,14] As the weight fraction of the homo-PAr increases in place of the pure PS-PAr block copolymer, in other words, as the block copolymerization ratio of the PAr in step 3 decreases, the ratio of the macroscopic PAr domains increases. Because the reactivity of the OH groups in both OH-PS-OH and bisphenol-A (BPA) is the same,[15,17] the block copolymerization ratio of the PAr is determined analogously by the ratio of $[-OH]_{PS}/[-OH]_{BPA}$ ratio (as in Fig. 5), which is equivalent to the mole fraction of the fed OH-PS-OH in step 3. As Mn (number average molecular weight) of the fed OH-PS-OH increases keeping the fed weight fraction constant or as the weight fraction of the fed HO-PS-OH increases keeping Mn of OH-PS-OH constant, the mole fraction of the fed OH-PS-OH in step 3 decreases. As a result, the block copolymerization ratio of PAr in step 3 decreases (Fig. 5). From the results that the scale of PAr domain size changes between run 2150 and 5075, the transition, from the microscopic to simultaneous micro and macroscopic phase separation, occurs at the PAr block
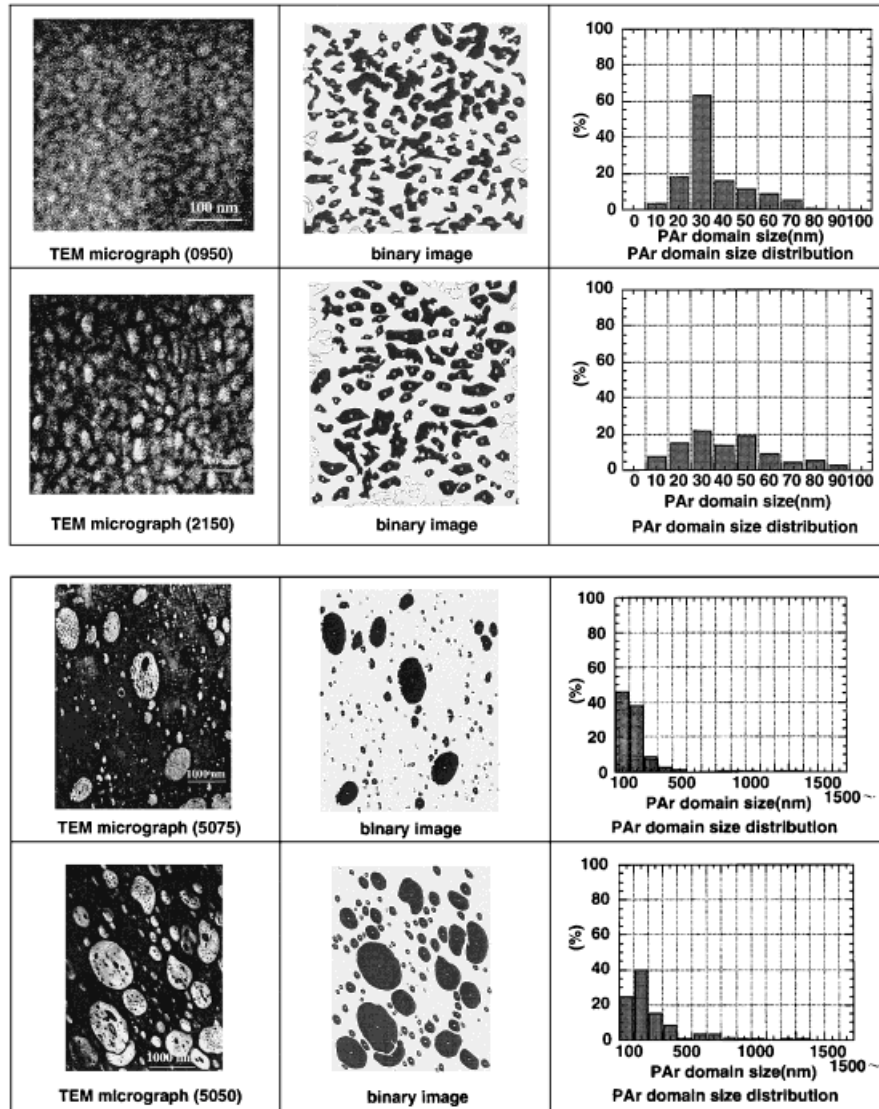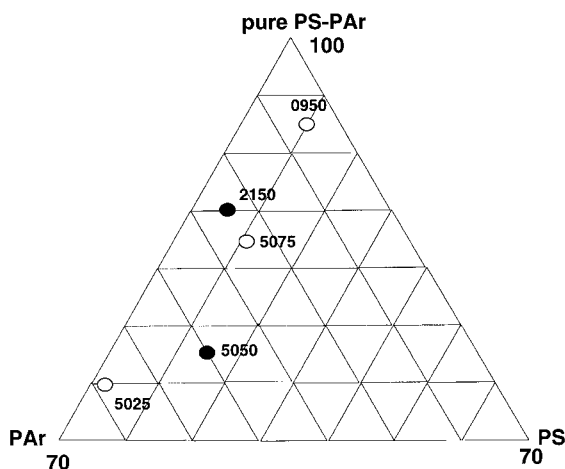
Figure 2 The TEM micrograph, its binary image, and PAr size distribution of run 0950 and 2150.

Figure 3 The TEM micrograph, its binary image, and PAr size distribution of run 5075, 5050, and 5025.

Figure 4 Weight fraction of the constituents in the PS-PAr block copolymers. ●, the experimental results; ○, the predictions by the kinetic simulation model.[14]

copolymerization ratio of around 50%. This means that the PAr domain size can be reduced to the microscopic scale by controlling the fed OH-PS-OH mole fraction more than around 0.016 in synthesizing the PS-PAr block copolymer, although some scattering are observed for run 5075 near this critical point.

The shape of the PAr domain for run 0950 and 2150 sample is poor in regularity. For run 5050 and 5075, the PAr domain looks circular whereas for run 5025 the PAr domains are highly ordered towards the flow direction. This signifies that the degree of PAr chain orientation increases with increasing PAr composition. This increase shifts the retained birefringence towards positive birefringence and this will be discussed later.
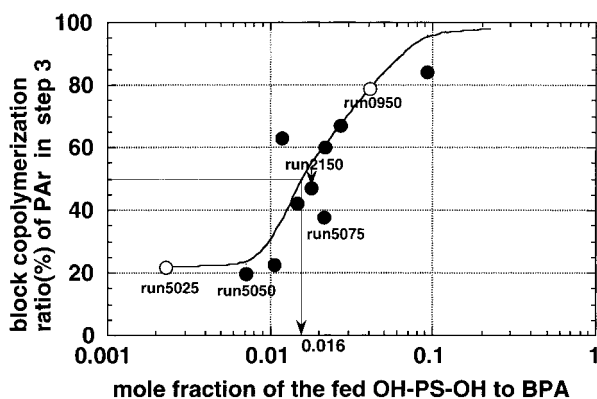
Figure 5 Relationship between mole fraction of the fed OH-PS-OH and block copolymerization ratio of PAr in step 3. ● and ○, the predicted curve by the simulation model.[14]
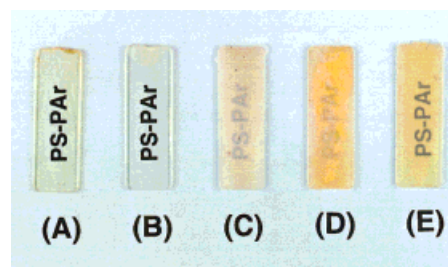
Figure 6 Transparency of the PS-PAr block copolymers. (A), (B), (C), (D), and (E) are run 0950, 2150, 5050, 5025, and 5075, respectively.

Transparency of the PS-PAr Block Copolymers

PAr domains dispersed in PS continuous matrix lead to light scattering because of large difference in the refractive index between PS and PAr:1.59 for PS,[18] and 1.61 for PAr,[19] respectively. The absorbance (α) of the light scattering of PAr domains is described by the refractive index difference, the size, and volume fraction of PAr domains and given by eq. (1)[20]:

$$\alpha = 2 \ \pi^3 (\Delta n_{PS/PAr}/n_{PS})^2 V_{PAr} \phi_{PAr}/\lambda^4 \qquad (1)$$

The transparency (T) of the passing beam is given by eq. (2):

$$T = k \ \exp(-\alpha \ d) \qquad (2)$$

where n_{PS}, $\Delta n_{PS/PAr}$, V_{PAr}, ϕ_{PAr}, λ, and d are the refractive index of PS, the refractive index difference between PS and PAr, volume of PAr domain, volume fraction of PAr domain, wavelength of the incident beam, and thickness of the specimen, respectively.

Figure 6 gives the transparency of the PS-PAr block copolymer specimens. Run 0950 and 2150 showed excellent transparency, whereas run 5025 was poor in transparency. Figures 7 shows how
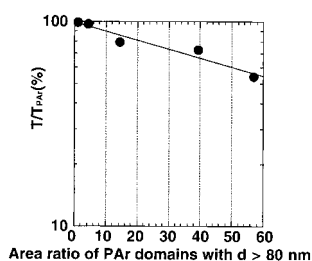
Figure 7 Relationship between area ratio of PAr domains with size larger than 80 nm and the transparency to the passing beam ($\lambda = 800$ nm).
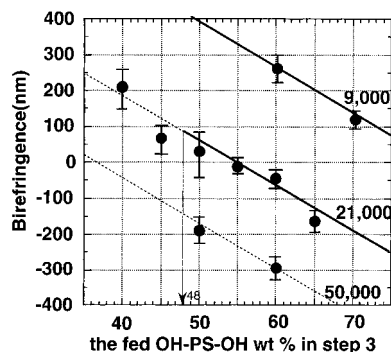
Figure 8 Birefringence of PS-PAr block copolymers as a function of weight fraction and Mn of the fed OH-PS-OH. $Mn_{\text{OH-PS-OH}}$ is shown on the curve.

the transparency depends upon the area ratio of PAr domains with the size larger than 80 nm (an order of magnitude smaller than the measured light wavelength) that represents $V_{\text{PAr}} \cdot \phi_{\text{PAr}}$ in eq. (1). To eliminate the effect of the reflection at the specimen surface, the transparency in Figure 7 is calibrated by that of PAr (U-100, Unitika Corp., Kyoto, Japan) specimen. The transparency decreases exponentially as the area ratio of the PAr domains increases, which may be due to the light scattering caused by PAr domains with the size of over 1/10 of the wavelength.

Considering these experimental results combined with these the previous discussions, we can conclude that: by controlling the fed OH-PS-OH mole fraction more than around 0.016 in the PS-PAr block copolymer preparation, the PAr domain size can be reduced down to smaller than about 100 nm. As a result, the PS-PAr block copolymers exhibit almost the same transparency as PAr in spite of the large difference in the refractive index between PS and PAr.

Birefringence of the PS-PAr Block Copolymers

Figure 8 shows the residual birefringence of the PS-PAr block copolymers as a function of weight fraction and Mn of the fed OH-PS-OH. The PS-PAr block copolymers show the residual birefringence depending not only on weight fraction but also on Mn of the fed OH-PS-OH. Based on the criteria in the previous discussion, the weight fraction region of the fed OH-PS-OH with good transparency, is estimated corresponding to Mn of the fed PS, as shown in Figure 8 (solid line).

The residual birefringence of the multicomponent polymer system is generally formulated by eq. (3)[21]:

$$\Delta n = \Sigma \phi_i f_i \Delta n_i^0 + \Delta n_F \qquad (3)$$

where Δn, ϕ_i, f_i, Δn_i^0, and Δn_F are the residual birefringence of the multicomponent polymer system, the volume fraction of polymer i, the orientation function of polymer i, the intrinsic birefringence of polymer i, and the form of birefringence, respectively. As in general Δn_F is negligible compared with the first term of eq. (3),[22] and Δn_F could be neglected. Thus if the molecular orientation of both PS and PAr is the same degree, the birefringence-free PS composition should be estimated to be around 64% by solving eq. (3) under the condition of $f_{\text{PS}} = f_{\text{PAr}}$, $\Delta n_{\text{PS}}^0 = -0.100$,[10] and $\Delta n_{\text{PAr}}^0 = 0.177$.[10] This birefringence-free condition should be valid for the miscible polymer blend system such as polyvinylidene fluoride and polymethyl methacrylate system[23] owing to its homogeneity in molecular orientations.

A certain deviation of the experimental results from the above estimation suggests that, owing to the phase separation, PS and PAr chain undergo inhomogeneous stress or relaxation history during the melt flow and solidification processes. As a result, the degree of molecular orientation in the specimens, for both PS and PAr chains, is different, i.e., $f_{\text{PS}} \neq f_{\text{PAr}}$.

When Mn of the fed OH-PS-OH is 50 000, the PS-PAr block copolymers exhibited negative birefringence even at the fed OH-PS-OH wt % of 50 and 60 wt % (Fig. 8). As shown in Figure 3 for run 5050 and 5075, the molecular orientation of PAr chain is fully relaxed in the fed PS wt % ranging from 50 to 75 wt %. This indicate that the degree of PS chain orientation is larger than that of PAr chain, i.e., $f_{\text{PS}} > f_{\text{PAr}}$ and resulting in the negative birefringence. This difference in the molecular orientation may be due to a large difference of the chain length between the PS matrices and the PAr domains.

The chain length of PAr domains and PS matrices could be estimated as follows. PAr domains should consist of PAr chains of pure PS-PAr block copolymer and homo-PAr obtained as a byproduct. From consideration of polymerization kinetics,[15] the PAr chain length of pure PS-PAr block copolymer is supposed to be the same as that of homo-PAr. Thus the chain length of PAr domain could be estimated by Mn of homo-PAr. On the other hand, because PS matrices should consist of PS chains of pure PS-PAr block copolymer and unreacted homo-PS, the chain length of PS matrices should be estimated by Mn of the fed OH-PS-OH.

As shown in Table I, for run 5050 and 5060, Mn of PAr domains can be estimated about 1/5 of that of the PS matrices. As the fed PS composition decreases keeping Mn of the fed OH-PS-OH 50 000, the degree of PAr chain orientation increases due to the increase of Mn of the PAr phase as shown for run 5025 of Figure 3 (for run 5025, Mn of PAr chain is estimated about 2 times larger than that of run 5050 as shown in Table I). The birefringence of PS-PAr block copolymer is expected to be zero at the fed OH-PS-OH wt % below 40 wt %. This composition deviates from the estimated range of the fed OH-PS-OH for good transparency.

On the other hand, when Mn of the fed OH-PS-OH is 9000, the situation is completely different. The PS-PAr block copolymer exhibited the positive birefringence even at the fed OH-PS-OH wt % > 64 wt %, indicating a higher degree of PAr chain orientation than that of PS chain, i.e., $f_{PS} < f_{PAr}$. This may be due to the fact Mn of the PAr domains is estimated almost the same as that of the PS phase as shown for run 0970 of Table I. In this case the fed PS wt % for optically homogeneous block copolymer is expected to be larger than 70 wt %.

When Mn of the fed OH-PS-OH is 21 000, the birefringence of the PS-PAr block copolymers changes from positive to negative as the fed OH-PS-OH wt % increases from 40 to 65 wt %. The PS-PAr block copolymer exhibited almost zero birefringence at around 55 wt % without any loss in transparency. At this fed OH-PS-OH wt % Mn of PAr phase is around 10 000 as shown for run 2155 in Table I.

To confirm the origin of the negative birefringence in the above discussions, the plate specimens of run 2160 were annealed at 423 K for 30 min. The annealing temperature is the intermediate between PS[18] and Par[19] glass transition temperatures. The preliminary annealing of OH-PS-OH (Mn = 21 000) and PAr (U-100, Unitika Corp., Kyoto, Japan) specimens showed that the morphology of the PS specimen was deformed leading to a decrease in their birefringence due to a relaxation of molecular orientations, whereas for PAr specimens its morphology was observed unchanged and its birefringence was nearly the same before and after the annealing. This suggests that under this annealing condition, molecular orientation of only PS chain is relaxed whereas molecular orientation of PAr chain is remaining the same. In Figure 9 the change in birefringence of run 2160 before and after the
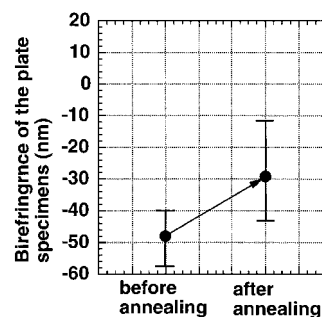
Figure 9 Birefringence change of run 2160 before and after annealing (323 K, 30 min).

annealing is shown. The birefringence of run 2160 after annealed shifted towards positive. This results signifies that the negative birefringence of the PS-PAr block copolymers is originated from the molecular orientation of PS chains.

However neither large deformation of morphology of the specimen as the OH-PS-OH specimens nor birefringence shift from minus to plus was observed after the annealing. This may be due to the following reason. From consideration of polymerization kinetics,[15] the pure PS-PAr block copolymer, for run 2160, has more than 80 wt % multitype block copolymer whose terminals of PS chains are both fixed by PAr chains. As a result, the orientation of PS chains could not be completely relaxed. Hence minus birefringence should be remained even after the annealing.

From the above results, PS and PAr chains in the PS-PAr block copolymers undergo inhomogeneous stress or relaxation history during the melt flow and solidification processes due to phase separation. As a result, the condition for optically homogeneous PS-PAr block copolymers is determined not only by PS composition but also by the balance between the degree of PS and PAr chain orientation, which are determined by the chain length or processing conditions. Under our experimental analysis, Mn and weight fraction of the fed OH-PS-OH around 20 000 and 55 wt %, respectively, are found to be the optimum condition for the PS-PAr block copolymer with zero birefringence and without any loss in transparency.

CONCLUSIONS

The relationship between the phase morphology and optical properties of the PS-PAr block co-

polymer synthesized in the scheme shown in Figure 1 has been studied. It is found that:

1. In the PS-PAr block copolymers, the PAr phase with higher melt viscosity forms dispersed domains in PS matrix with lower melt viscosity over the wide composition range from PS/PAr = 25/75 to 75/25.

2. The PAr domain size depends on the block copolymerization ratio of PAr, which is postulated to be the same as the mole fraction of the fed OH-PS-OH in step 3 in the reaction scheme of Figure 1. By controlling the mole fraction of the fed OH-PS-OH more than ca. 0.016 in step 3, the PAr domain size can be made smaller down to 100 nm. As a result, the PS-PAr block copolymers exhibit almost the same transparency as PAr in spite of a large difference in the refractive index between PS and PAr.

3. The birefringence-free condition for the PS-PAr block copolymer is determined not only by PS composition but also by the balance between the degree of PS and PAr chain orientation. This is because the PS and PAr chains in the PS-PAr block copolymers undergo inhomogeneous stress or relaxation history during melt flow and solidification processes due to the phase separation. Controlling Mn and weight fraction of the fed OH-PS-OH are around 20 000 and 55 wt %, respectively; for synthesizing PS-PAr block copolymer, the resultant PS-PAr block copolymer exhibits almost zero birefringence without any loss in transparency.

4. Considering above all conclusive remarks comprehensively, our developed PS-PAr block copolymer could have a great potential to be controlled for optical applications, such as a substrate of optical disks or optical lenses.

REFERENCES

1. Ward, I. M. Structure and Properties of Oriented Polymers; John Wiley & Sons, 1975.
2. Marchant, A. B. Proc SPIE 1983, 421, 43.
3. Gossink, R. G.; Buning, G. H. W.; Wimberger-Friedl, R. Integr Fundam Polym Sci Tschnol 1989, 3, 355.
4. Emmelui, M.; Pawlowski, G.; Vollmann, H. W. Angre Chem 1989, 101, 1475.
5. Wimberger-Friedl, R. Polym Eng Sci 1990, 30, (14), 813.
6. Rohrbach, P.; Heitz, T.; Keul, H.; Hocker, H. Makromol Chem 1993, 194, 1627.
7. Siebourg, W.; Schmid, H.; Rateike, F. M.; Anders, S.; Grigo, U.; Lower, H. M. Polym Eng Sci 1990, 30, (18), 1133.
8. Pisipati, R. M.; Newcome, J. M.; Lower, H. M. Plastic Eng 1995, (4), 33.
9. Toyota, T.; Yasue, K. Plastics 1985, 36, 116.
10. Tanaka, T.; Inoue, T. J Non-Cryst Solids 1991, 36, (2), 781.
11. Eguiazabal, J. I.; Calahorra, M. E.; Cortazar, M. M.; Iruin, J. J. Polym Eng Sci 1984, 24, 608.
12. Hahn, B. R.; Wendorf, J. H. Polymer 1985, 26, 1619.
13. Ohishi, H.; Kimura, M. Nippon Steel Technical Report 1993, 53, 39.
14. Ohishi, H.; Ohwaki, T.; Nishi, T. J Polym Sci Part A, Polym Chem 1998, 36, 2839.
15. Ohishi, H.; Nishi, T. J Polym Sci Part A Polym Chem 2000, 38, 299.
16. Tanaka, H.; Hashimoto, T. Polym Commun 1988, 29, 211.
17. Niwa, M.; Hayashi, T.; Matsumoto, T. J Macromol Sci Chem 1986, A23, 433.
18. Landry, C. J. T.; Yang, H.; Machell, J. S. Polymer 1991, 32, 44.
19. Catalog of U-polymer, Unitika Corporation.
20. Hayakawa, S. Rikougaku-kisokouza. Asakura IPC 1976, 24.
21. Saito, H.; Takahashi, M.; Inoue, T. J Polym Sci Part B 1987, 25, 1629.
22. Inoue, T.; Saito, H. Kinouzairyo 1987, 3, 21.
23. Saito, H.; Takahashi, M.; Inoue, T. J Polym Sci Part B 1988, 26, 1761.